




# Multidisciplinary modeling and surrogate assisted optimization for satellite constellation systems

Renhe Shi<sup>1,2</sup> · Li Liu<sup>1,2</sup> · Teng Long<sup>1,2</sup>  · Yufei Wu<sup>1,2</sup> · G. Gary Wang<sup>3</sup>

Received: 12 April 2018 / Revised: 3 June 2018 / Accepted: 13 June 2018  
© Springer-Verlag GmbH Germany, part of Springer Nature 2018

## Abstract

Satellite constellation system design is a challenging and complicated multidisciplinary design optimization (MDO) problem involving a number of computation-intensive multidisciplinary analysis models. In this paper, the MDO problem of a constellation system consisting of small observation satellites is investigated to simultaneously achieve the preliminary design of constellation configuration and the satellite subsystems. The constellation is established based on Walker- $\delta$  configuration considering the coverage performance. Coupled with the constellation configuration, several disciplines including payload, power, thermal control, and structure are taken into account for satellite subsystems design subject to various constraints (i.e., ground resolution, power usage, natural frequencies, etc.). Considering the mixed-integer and time-consuming behavior of satellite constellation system MDO problem, a novel sequential radial basis function (RBF) method using the support vector machine (SVM) for discrete-continuous mixed variables notated as SRBF-SVM-DC is proposed. In this method, a discrete-continuous variable sampling method is utilized to handle the discrete variables, i.e., the number of orbit planes and number of satellites, in the satellite constellation system MDO problem. RBF surrogates are constructed and gradually refined to represent the time-consuming simulations during optimization, which can efficiently lead the search to the optimum. Finally, the proposed SRBF-SVM-DC utilized to solve the satellite constellation system MDO problem is compared with a conventional integer coding based genetic algorithm (ICGA). The results show that SRBF-SVM-DC significantly decreases the system mass by about 28.63% subject to all the constraints, which greatly reduces the cost of the satellite constellation system. Moreover, the computational budget of SRBF-SVM-DC is saved by over 85% compared with ICGA, which demonstrates the effectiveness and practicality of the proposed surrogate assisted optimization approach for satellite constellation system design.

**Keywords** Satellite constellation system · Surrogate-based analysis and optimization · Multidisciplinary design optimization · Mix-integer optimization

## 1 Introduction

Constellations of satellites have received growing interest in recent years due to their merits in Earth and space observation,

---

Responsible Editor: Somanath Nagendra

---

✉ Teng Long  
tenglong@bit.edu.cn

<sup>1</sup> School of Aerospace Engineering, Beijing Institute of Technology, 5 South Zhongguancun Street, Haidian District, Beijing 100081, China

<sup>2</sup> Key Laboratory of Dynamics and Control of Flight Vehicle, Ministry of Education, School of Aerospace Engineering, Beijing Institute of Technology, 5 South Zhongguancun Street, Haidian District, Beijing 100081, China

<sup>3</sup> Product Design and Optimization Laboratory, School of Mechatronic Systems Engineering, Simon Fraser University, Surrey, BC V3T 0A3, Canada

guidance and navigation, and telecommunication. In constellations, multiple satellites work cooperatively for specific space missions to significantly enhance the capability and reliability of space systems. To achieve different space missions, several fundamental constellations have been developed in the past decades, e.g., Walker constellations (Walker 1977), Flower constellations (Mortari et al. 2004), etc. Many of them have been successfully applied in practice such as the famous GPS and Iridium. Based on those works, the existing studies of constellation design mostly focused on optimizing the configuration parameters (e.g., altitude, inclination, and number of satellites) or extending the design framework of constellation to acquire better system indexes, e.g., coverage performance, geometric dilution of precision (GDOP), etc. For instances, Pu (Pu et al. 2017) designed a small satellite constellation with maximum target observation time through a robust NSGA-II based multi-objective optimization method.

Arnas (Arnas et al. 2018) investigated the methodology of 2D Necklace Flower Constellations based on the 2D Lattice Flower constellation, which is flexible for configuration design and optimization. Casanova (Casanova et al. 2014) utilized an enhanced particle swarm optimization (PSO) algorithm to obtain the flower constellation with the best GDOP considering different numbers of satellites. Asgarimehr (Asgarimehr and Hossainali 2014) used genetic algorithm to optimize the geometry of navigation constellation system considering different design criteria. Note that the design of constellation is subject to the capability of satellite subsystems (e.g., satellite mass and power budgets, and payload performance) in engineering practices, and the satellite subsystems design also needs to be adaptive to a given constellation configuration. Hence, the satellite constellation system design is practically a multidisciplinary design optimization (MDO) problem (Budianto 2000), where it is preferable to design the constellation configuration and satellite subsystems simultaneously. In this way, the inter-couplings between the constellation configuration and satellite subsystems can be fully exploited to improve the design quality and performance of the aerospace system. However, most aforementioned literatures simply regarded a complex satellite system as geometry nodes within a constellation network, where the parameters of satellite subsystems are fixed or even not considered.

Multidisciplinary design optimization was defined as “a methodology for the design of complex engineering systems and subsystems that coherently exploits the synergy of mutually interacting phenomena” (Sobieski 1993), which has been widely applied in aerospace system design (Sobieszczanski-Sobieski and Haftka 1997; Martins and Lambe 2013). However, the satellite constellation system MDO problems face the challenge of enormous computational cost due to the use of time-consuming simulation models, e.g., finite element analysis (FEA) model of satellite structures. Hence, the evolutionary algorithms (e.g., GA and PSO) for conventional constellation configuration design are unsuitable for optimizing the computation-intensive satellite constellation system MDO problems, because these methods generally require an

excessive number of function evaluations to search the optimum. To reduce computational cost, surrogate-based analysis and optimization (SBAO), or metamodel-based design optimization (MBDO) (Jin et al. 2001; Wang and Shan 2007; Forrester and Keane 2009; Queipo et al. 2005) have been widely employed. In SBAO, a surrogate is constructed to replace the expensive analysis model for optimization. And the surrogates are usually refined via progressive sampling based on certain criteria to improve the approximation accuracy during the optimization, which gradually leads the search to the optimum. In the literatures, a number of SBAO methods have been developed in recent years (Wang et al. 2004; Long et al. 2015; Shi et al. 2016), and some of them have been successfully applied for aerospace system design optimization problems, e.g., all-electric GEO satellite MDO problem (Shi et al. 2017), maneuver satellite system MDO problem (Huang et al. 2014), and emergency libration point orbits transfer problem (Wang 2017). In view of the expensive black-box simulations in MDO of satellite constellation systems, it is valuable and promising to apply SBAO to improve the overall system performance and save computational cost. However, few studies on surrogate assisted optimization for satellite constellation system design have been reported.

To address the challenges of satellite constellation system multidisciplinary design optimization and associated expensive computational cost, this paper investigates the satellite constellation system MDO problem using surrogates. A novel SBAO method termed SRBF-SVM-DC is developed based on our previously proposed sequential radial basis function method using support vector machine (SRBF-SVM) (Shi et al. 2016), which is tailored to efficiently solve the satellite constellation system MDO problem including both continuous and discrete variables. The remainder of this paper is organized as follows. The studied satellite constellation system MDO problem is introduced in Section 2, where the configuration is based on Walker- $\delta$  constellation and the satellite system involves four disciplines. The disciplinary analysis models of the constellation and satellite system are detailed in Section 3. The algorithm of SRBF-SVM-DC is described in Section 4. The application of the proposed SRBF-SVM-DC to solve the satellite constellation system MDO problem is

**Fig. 1** Illustration of Earth observation satellite configuration

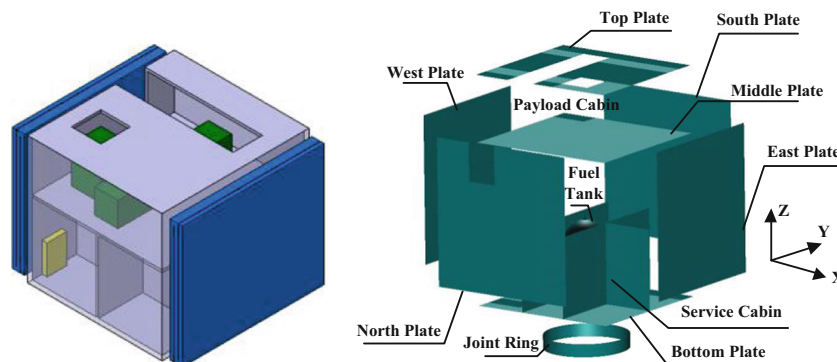
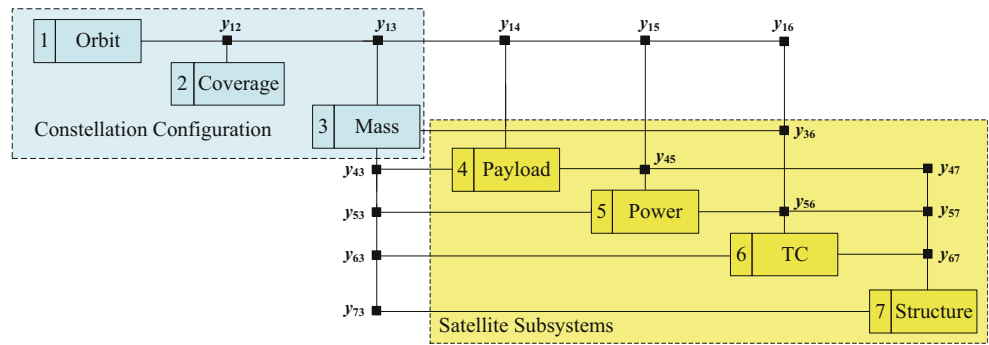


**Fig. 2** Design structure matrix of satellite constellation MDO problem



explained in Section 5 and compared with a conventional integer-coding-based genetic algorithm (ICGA). Finally, the conclusions are summarized in Section 6.

## 2 Description of satellite constellation system MDO problem

In this study, a coverage constellation consisting of small satellites is established to achieve the Earth observation mission. Considering the coupling relationships among different disciplines of the satellite constellation system, the configuration of the constellation and design parameters of the satellite subsystems are simultaneously optimized to enhance the system performance. In this work, the constellation configuration is established based on Walker- $\delta$  constellation. In Walker- $\delta$  constellation, the ascending nodes of the orbit planes are uniformly distributed around the reference plane (i.e., the equator for most cases), and the satellites are uniformly distributed within the orbital planes at the same inclination (Walker 1977). The small Earth observation satellite in the constellation is a cuboid with the dimension of 1200(X)  $\times$  1100(Y)  $\times$  900(Z) mm, whose configuration is graphically illustrated in Fig. 1. The solar arrays are installed on the North/South surfaces of the satellite to provide power, and a CCD camera is equipped in the payload cabin of the satellite system to implement the observation mission. Other devices (e.g., the batteries and control systems) are mounted in the service cabin.

The satellite constellation system MDO problem can be therefore divided into two parts, i.e., the design optimization

of constellation configuration and the satellite subsystems. The coupling relationships among different disciplines are graphically organized in a design structure matrix (DSM) as shown in Fig. 2.

In the DSM, the diagonal elements are the disciplines, and the black squares represent the coupling variables as listed in Table 1. In this work, the constellation configuration consists of the orbit, coverage, and mass disciplines, which determines the constellation geometry, observation coverage ratio, and entire mass of the system respectively. The satellite subsystems involve the payload, power, thermal control (TC), and structure disciplines. Other disciplines such as attitude control (AC) and communication can follow the mature design of existing small satellites, which are not included in the MDO problem and simply regarded as the fixed mass budget on the satellite platform in the preliminary design phase. For instances, the satellite communication is in S-band, and the satellite system is three-axis-stabilized using three magnetorquers and hydrazine propulsion for attitude control and orbit change maneuvers. In the preliminary design phase, the parameters of payload, power, TC, and structure subsystems are assumed to be identical for the satellites in the constellation system.

Since the decrease of weight can directly save launch cost, the objective of the MDO problem in this paper is to minimize the total mass of the satellite constellation system (i.e., the total mass of all the satellites) for saving the overall cost of the system, subject to engineering constraints such as coverage performance. In this work, both continuous and discrete variables (e.g., orbit altitude, number of satellites) need to be

**Table 1** Coupling variables of different disciplines

Symbol	Definition	Symbol	Definition
$y_{12}$	Constellation parameters	$y_{45}$	Power budget of payload
$y_{13}$	Total number of satellites	$y_{47}, y_{43}$	Mass budget of payload
$y_{14}$	Orbit altitude	$y_{56}$	Satellite power usage
$y_{15}$	Incidence angle of sunlight; maximum eclipse time	$y_{57}, y_{53}$	Mass budget of power subsystem
$y_{16}$	Incidence angle of sunlight; maximum lightening time	$y_{67}, y_{63}$	Mass budget of TC subsystem
$y_{36}$	Satellite mass	$y_{73}$	Structural mass

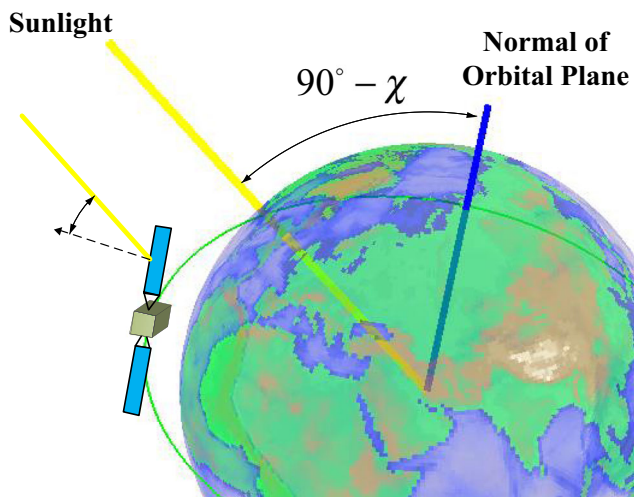


Fig. 3 Illustration of sunlight incidence angle

optimized subject to a number of engineering constraints (e.g., payload resolution, natural frequency of structure). The detailed multidisciplinary modeling process and mathematical formulation of the satellite constellation system MDO problem are presented in Section 3.

### 3 Multidisciplinary modeling for satellite constellation systems

In this section, the multidisciplinary modeling processes for the satellite constellation MDO problem are detailed. Based on the disciplinary models, the mathematical formulation of the MDO problem is presented.

#### 3.1 Orbit discipline

For the Walker- $\delta$  constellation in this paper, the semi-axis, inclination, and eccentricity (i.e., zero for circular orbits in this study) of different orbits are equal, while the orbit planes are uniformly distributed along the equator with respect to the right ascension of ascending node (RAAN). In the orbit discipline, the constellation parameters including the altitude, inclination, and the RAAN of the first orbit plane are designed to establish the fundamental configuration of constellation, which is the basis for satellite constellation system modeling and analysis. In this study,

the modified equinoctial elements (MEE) (Walker 1986) are employed to establish the orbit model due to its desirable property of no practical singularity. The MEE are given by (1)

$$\begin{cases} p = a(1-e^2) \\ f = e \cos(\omega + \Omega) \\ g = e \sin(\omega + \Omega) \\ h = \tan(i/2)\cos(\Omega) \\ k = \tan(i/2)\sin(\Omega) \\ L = \Omega + \omega + \nu \end{cases} \quad (1)$$

where  $a$ ,  $e$ ,  $i$ ,  $\Omega$ ,  $\omega$ , and  $M$  are the classical Keplerian orbital elements. The constellation dynamics model in terms of MEE is formulated in (2) (Ghosh and Coverstone 2015):

$$\begin{cases} \frac{dp}{dt} = \sqrt{\frac{p}{\mu}} \frac{2p}{w} f_T \\ \frac{df}{dt} = \sqrt{\frac{p}{\mu}} \left( f_R \sin(L) + [(1+w)\cos(L) + f] \frac{f_T}{w} (h \sin(L) - k \cos(L)) \frac{gf_N}{w} \right) \\ \frac{dg}{dt} = \sqrt{\frac{p}{\mu}} \left( f_R \cos(L) + \sqrt{\frac{p}{\mu}} [(1+w)\sin(L) + f] \frac{f_T}{w} (h \sin(L) - k \cos(L)) \frac{gf_N}{w} \right) \\ \frac{dh}{dt} = \sqrt{\frac{p}{\mu}} \frac{s^2 f_N}{2w} \cos(L) \\ \frac{dk}{dt} = \sqrt{\frac{p}{\mu}} \frac{s^2 f_N}{2w} \sin(L) \\ \frac{dg}{dt} = \sqrt{\mu p} \left( \frac{w}{p} \right)^2 + \frac{1}{w} \sqrt{\frac{p}{\mu}} (h \sin(L) - k \cos(L)) f_N \end{cases} \quad (2)$$

where  $f_R$ ,  $f_T$ , and  $f_N$  are respectively the disturbance accelerations expressed in the RTN coordinate system. In the preliminary design phase, it is assumed that the dynamics model only considers the disturbance accelerations due to the J2 zonal harmonics of non-spherical gravitational potential, which is given in (3) (Ghosh and Coverstone 2015)

$$a_{J2} = \begin{bmatrix} -\frac{3J_2\mu R_e^2}{2r^4} \left( 1 - 12 \frac{(h \sin(L) - k \cos(L))^2}{s^4} \right) \\ -\frac{12J_2\mu R_e^2}{r^4} \left( \frac{(h \sin(L) - k \cos(L))(h \cos(L) + k \sin(L))}{s^4} \right) \\ -\frac{6J_2\mu R_e^2}{r^4} \left( \frac{(h \sin(L) - k \cos(L))(1 - k^2 - h^2)}{s^4} \right) \end{bmatrix} \quad (3)$$

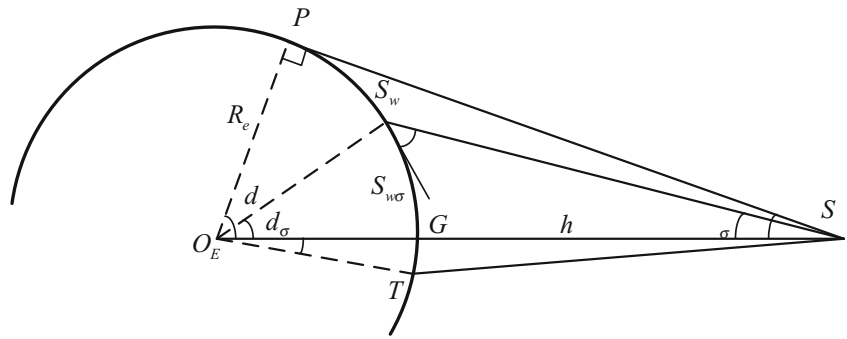
where  $[x, y, z]$  is the position of the satellite in ECI,  $R_e = 6378$  km is the radius of the Earth,  $J_2 = 1.082626 \times 10^{-3}$  is the zonal harmonics coefficient, and  $\mu = 398,600.5 \text{ km}^3 \text{ s}^{-2}$  is the Earth's gravitational constant.

Given the inclination and RAAN of the orbit, the incidence angle of sunlight  $\chi$  to the orbit plane as shown in Fig. 3 is

Table 2 Design variables of orbit discipline

Parameter	Description	Symbol	Unit	Range
Orbit altitude	Design variable (continuous)	$h$	km	[500,1500]
Orbit inclination	Design variable (continuous)	$i$	Deg	[30,60]
RAAN of the first orbit plane	Design variable (continuous)	$\Omega_o$	Deg	[0,30]
Number of orbit planes	Design variable (discrete)	$P$	–	[2,3,4,5,6]
Number of satellites in each orbit plane	Design variable (discrete)	$S$	–	[1,2,3,4]

**Fig. 4** Coverage model of a single observed point



computed by (4) (Xi 2003):

$$\sin(\chi) = \cos(\alpha_S)\sin(i)\sin(\Omega) + \cos(\Omega)\cos(\varepsilon)\sin(i)\sin(\alpha_S) - \cos(i)\sin(\varepsilon)\sin(\alpha_S) \quad (4)$$

where  $\varepsilon = 23.5^\circ$  is the obliquity of the ecliptic, and  $\alpha_S$  is the celestial longitude of the sun. To simplify the analysis for preliminary design, the solar arrays of the satellite are assumed to be consistently perpendicular to the orbital plane and point to the sunlight. Hence, the incidence angle of sunlight to the solar arrays is approximately equal to  $\chi$  as shown in Fig. 3. As for circular orbit, the orbit period  $T$ , lightning factor  $K_s$ , and the eclipse factor  $K_e$  of the satellite are given by (5) (Xi 2003). The maximum  $K_s$  and  $K_e$  over the year are determined as the coupling input of the TC discipline and power discipline respectively. The design variables of the orbit discipline are summarized in Table 2.

$$\begin{aligned} T &= 2\pi\sqrt{\frac{(R_e + h)^3}{\mu}} \\ K_s &= \frac{1}{2} + \arcsin\left(\frac{\sqrt{2R_e h + h^2}}{(R_e + h)\cos(\chi)}\right) / \pi \\ K_e &= \frac{1}{2} - \arcsin\left(\frac{\sqrt{2R_e h + h^2}}{(R_e + h)\cos(\chi)}\right) / \pi \end{aligned} \quad (5)$$

### 3.2 Coverage discipline

In the coverage discipline, the coverage ratio of the constellation for the Earth region of interests is calculated as a local constraint of the MDO problem. The coverage analysis model of a single observed point is graphically illustrated in Fig. 4, where  $S$  represents the satellite and  $G$  is the associated satellite bottom point. In view of the minimum observation angle on the ground  $\sigma$  (i.e.,  $10^\circ$  in this study), the coverage angle  $d_\sigma$ , central angle  $\alpha_\sigma$ , and coverage width  $S_{w\sigma}$  are presented in (6) (Wertz 1999).

$$d_\sigma = \arccos\left(\frac{R_e \cos(\sigma)}{R_e + h}\right) - \sigma \alpha_\sigma = \pi/2 - d_\sigma - \sigma S_{w\sigma} = 2R_e \cdot d_\sigma \quad (6)$$

Given the longitude and latitude of the ground observed point  $T$  (i.e.,  $\lambda_W$  and  $\varphi_W$  respectively), the field angle for the Earth center between  $S$  and  $T$  is determined by (7) (Wu et al. 2013a):

$$\cos(\theta) = \sin(\varphi_W)\sin(\varphi_S) + \cos(\varphi_W)\cos(\varphi_S)\cos(\lambda_W - \lambda_S) \quad (7)$$

where  $\lambda_S$  and  $\varphi_S$  are the longitude and latitude of  $G$  respectively. If  $\theta \leq d_\sigma$ , the ground observed point is covered by the

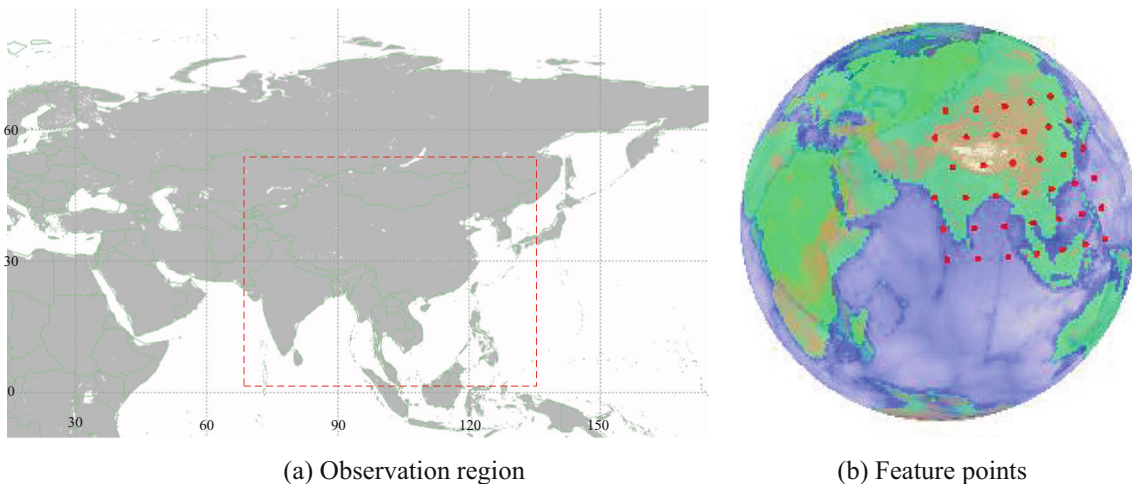


**Fig. 5** Illustration of observation region and feature points

**Table 3** Design variables and constraints of payload discipline

Parameters	Description	Symbol	Unit	Range
Aperture size of payload	Design variable (continuous)	$D_p$	mm	[5,15]
Focus length of payload	Design variable (continuous)	$f_p$	mm	[10,50]
Ground pixel resolution of payload	Constraint	$R_p$	m	$\leq 250$
SNR of payload	Constraint	$SNR$	–	$\geq 500$

satellite. As for the observation region, a number of feature points are generated within the region to identify if the region is covered by the constellation according to (7). To achieve good distribution quality, the margins of longitude and latitude between the adjacent feature points are calculated through (8) (Dai and Wang 2009):

$$\begin{cases} \Delta\lambda = \Delta l / (R_e \cos(\varphi)) \\ \Delta\varphi = \Delta l / R_e \end{cases} \quad (8)$$

where  $\Delta l$  is the length of ground arc between the adjacent feature points, and  $\varphi$  is the latitude of the feature point. In the preliminary design,  $\Delta l$  is assumed to be 500 km to make a trade-off between the coverage analysis accuracy and simulation cost. The associated longitude and latitude of the feature points are then given by (9)

$$\begin{cases} \lambda_i = \lambda_{\min} + i\Delta\lambda & i = 0, 1, \dots, n \\ \varphi_j = \varphi_{\min} + j\Delta\varphi & j = 0, 1, \dots, m \end{cases} \quad \begin{cases} \lambda_i \in [\lambda_{\min}, \lambda_{\max}] \\ \varphi_j \in [\varphi_{\min}, \varphi_{\max}] \end{cases} \quad (9)$$

where  $\lambda_{\min}$ ,  $\varphi_{\min}$  and  $\lambda_{\max}$ ,  $\varphi_{\max}$  are respectively the lower and upper bounds of longitude and latitude of the region to be observed. In this work, the region to be observed on the Earth is 73°E~135°E and 3°N~53°N as illustrated in Fig. 5 (a), and the dots in Fig. 5 (b) represent the feature points in the observation region.

The coverage ratio of the constellation for the region of interests is defined by (10) (Dai and Wang 2009):

$$C_R = \frac{\sum_{i=1}^n T_i / n}{T_{\text{simulation}}} \quad (10)$$

where  $n$  is the number of feature points,  $T_i$  is the time of the  $i$ -th feature point being covered by one or multiple satellites, and  $T_{\text{simulation}}$  is the total simulation time.  $C_R$  indicates the

global or local coverage performance of the constellation, which generally increases as the orbit altitude grows. The coverage ratio is output as the local constraint of the coverage discipline, which should be no less than 80% as for the studied satellite constellation system in this paper.

### 3.3 Mass discipline

Given the number of orbit planes  $P$  and the number of satellites in each plane  $S$ , the entire mass of the satellite constellation system  $M_{\text{system}}$  is determined according to (11).

$$M_{\text{system}} = (m_{\text{payload}} + m_{\text{power}} + m_{\text{thermal}} + m_{\text{structure}} + m_{\text{others}}) \times S \times P \quad (11)$$

In (11),  $m_{\text{payload}}$ ,  $m_{\text{power}}$ ,  $m_{\text{thermal}}$ , and  $m_{\text{structure}}$ , are the mass budgets of the payload, power, TC, and structure subsystems respectively, which are determined by the associated disciplinary models.  $m_{\text{others}} = 198$  kg (Wu et al. 2013a) is the other fixed mass budget of the satellite including communication subsystem, attitude control (AC) subsystem, etc. The entire mass of the system is output as the objective of the MDO problem, which should be minimized.

### 3.4 Payload discipline

The payloads of satellite in the constellation can be remote sensing equipments (e.g., CCD cameras and SAR), telecommunication devices (e.g., antennas and transponders), and so on. In this work, the payload of the satellite is a 4-band CCD camera with the spectrum range from 0.45~0.52  $\mu\text{m}$ , 0.52~0.59  $\mu\text{m}$ , 0.61~0.69  $\mu\text{m}$ , and 0.76~0.89  $\mu\text{m}$  respectively. In the payload discipline, the aperture size  $D$  and focus length  $f$  of the CCD camera are designed to achieve the sizing

**Table 4** Design variables and constraints of power discipline

Parameter	Description	Symbol	Unit	Range
Area of solar arrays	Design variable (continuous)	$A_s$	$\text{m}^2$	[3,8]
Battery capacity	Design variable (continuous)	$C_s$	Ah	[20,80]
Depth of discharge	Constraint	–	–	$\leq 0.3$
Power surplus	Constraint	$W$	W	$\geq 0$

**Table 5** Design variable and constraint of TC discipline

Parameter	Description	Symbol	Unit	Range
Area of radiator	Design variable (continuous)	$A_R$	$m^2$	[0.5,1.08]
Maximum temperature	Constraint	$T_0$	K	$\leq 303.15$

of payload subsystem. Given the altitude of satellite and the focus length, the ground pixel resolution  $R_p$  of the payload is determined by (12) (Wu et al. 2013a):

$$R_p = \frac{hd}{f} \tag{12}$$

where  $d$  is the size of pixel of the CCD camera.  $R_p$  generally represents the minimum size of target that could be observed by the payload, which is proportional to the altitude of orbit.

Besides the resolution, the signal to noise ratio (SNR) of the payload is defined in (13) (Chen 2003). In the equation,  $V_n$  is the noise voltage of the payload,  $V_s$  is the signal voltage,  $F = f/D$  is focus length over the aperture size,  $\rho(\lambda) = 0.5$  is the ground reflection ratio,  $\tau_a(\lambda) = 0.8$  and  $\tau_0(\lambda) = 0.75$  are the transmittance of atmosphere and optical devices respectively,  $S_0 = 1353 \text{ W/m}^2$  is the solar constant, and  $\Delta\lambda$  is the bandwidth of the associated spectrum band (Chen 2003).

$$SNR = \frac{V_s}{V_n}, V_s = \frac{1}{4F^2} \rho(\lambda)\tau_a(\lambda)\tau_0(\lambda)S_0\Delta\lambda \tag{13}$$

Given the aperture size  $D$  and focus length  $f$ , the mass and power of the payload is sized via the subscale model according to (Wu et al. 2013a) as shown in (14):

$$\begin{aligned} m_{\text{payload}} &= \rho_m \cdot 1600 \cdot D^2 \cdot f \\ P_{\text{payload}} &= \rho_p \cdot 1600 \cdot D^2 \cdot f \end{aligned} \tag{14}$$

where  $\rho_m = 10^{-3} \text{ kg/mm}^3$  and  $\rho_p = 3.7 \times 10^{-3} \text{ W/mm}^3$  are respectively the mass and power densities of the payload in this study. The estimated mass and power of the payload are output to the power, TC, and structure disciplines. For the studied satellite constellation system in this paper, the design variables and constraints of the payload discipline are summarized in Table 3 based on the system design indexes provided by (Wu et al. 2013a).

### 3.5 Power discipline

The area of solar arrays and capacity of battery are designed in the power discipline to obtain the overall surplus power of the satellite and discharge depth of battery, which are output as the local constraints of the MDO problem. The beginning-of-life power ( $P_{BOL}$ ) of the satellite is given in (15) (Shi et al. 2017):

$$P_{BOL} = S_0 X_i X_s X_e X_0 A_S \eta F_c (\beta_p \Delta T + 1) \cos(\chi) \tag{15}$$

where  $X_i = 0.95$ ,  $X_s = 0.9637$ ,  $X_e = 1$ , and  $X_0 = 0.98$  are the correction factors,  $A_S$  is the area of the solar arrays,  $\eta = 0.28$  is the photoelectric conversion efficiency of the solar cell,  $F_c = 0.98$  is the solar array loss coefficient,  $\beta_p$  is the power temperature coefficient and  $\beta_p \Delta T + 1 = 0.826$  in this study, and  $\chi$  is the incident angle of sunlight output by the orbit discipline.

In this study, the required power of the satellite is estimated by (16):

$$P_N = \frac{P_0 \cdot T + P_{\text{payload}} \cdot T_{\text{payload}} + P_{\text{thermal}} \cdot T_e}{T - T_e} \tag{16}$$

where  $P_0 = 167 \text{ W}$  is the long-term power usage of the satellite,  $T_{\text{payload}} = 600 \text{ s}$  is the working time of the payload in each orbit period, and  $P_{\text{thermal}} = 60 \text{ W}$  is the power usage of TC subsystem during the eclipse. The surplus power of the satellite is then calculated by (17):

$$g_w = (1 - d_y)^{L_t} \cdot P_{BOL} - (1 + 5\%) \cdot P_N \tag{17}$$

where  $L_t = 5$  years is the on-orbit lifetime of the satellite, and  $d_y = 2.2\%$  is the annual power degradation of the solar arrays in LEO. To provide sufficient power for the satellite system, the surplus power  $g_w$  needs to be positive in the design.

When the satellite is in the shadow of the Earth, the storage battery group of the satellite has to provide sufficient power for the satellite. The depth of discharge (DOD) for the battery is defined as the ratio of its discharged capacity  $C$  to its rated capacity  $C_s$  as shown in (18) (Shi et al. 2017), where  $V_{DB} = 36 \text{ V}$  is the battery voltage. The maximum DOD should be restricted to a 30% level to prolong the life of battery according to (Wu et al. 2013a).

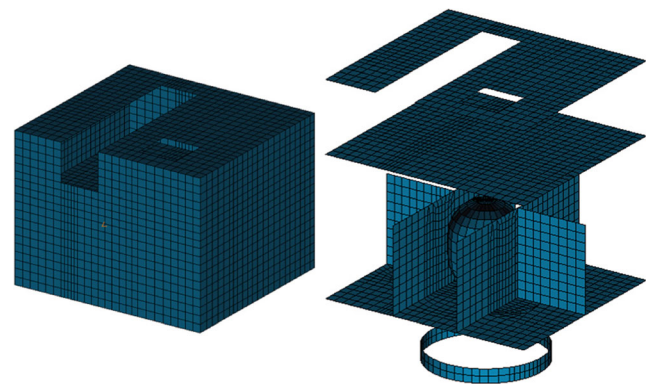


**Fig. 6** FEA model of the satellite

**Table 6** Design variables and constraints of structure discipline

Parameter	Description	Symbol	Unit	Range
Thickness of honeycomb core	Design variable (continuous)	$T_H$	mm	[7,13]
Thickness of the ply	Design variable (continuous)	$T_P$	mm	[0.07,0.13]
1st order bending frequency about X axis	Constraint	$f_X$	Hz	$\geq 20$
1st order bending frequency about Y axis	Constraint	$f_Y$	Hz	$\geq 20$

$$DOD = C/C_s C = (P_0 \cdot T_e + P_{\text{thermal}} \cdot T_e) / V_{DB} \quad (18)$$

Given the area of solar arrays  $A_s$  and the capacity of battery  $C_s$ , the mass of the power subsystem are estimated by (19):

$$m_{\text{power}} = \rho_{sa} A_s + C_s \cdot V_{DB} / \gamma_b \quad (19)$$

where  $\rho_{sa} = 2.83 \text{ kg/m}^2$  is the areal density of solar arrays, and  $\gamma_b = 39.6 \text{ kJ/kg}$  is the specific energy of the battery.

The design variables and constraints of the power discipline are summarized in Table 4.

### 3.6 Thermal control discipline

In the thermal control (TC) discipline, the radiators are sized to control the temperature inside the satellite in the sunlight area. In this work, the small satellite is encapsulated by multilayer insulation (MIL) blankets on the surfaces to reduce the influence of external heat flux, and the radiators are mounted on the south/north faces of the satellite. Assuming that the infrared radiation flow, reflection heat flow of the Earth, and the fluctuation of sunlight constant over the year are ignored for the preliminary design phase, the external heat flux of the satellite is calculated by (20) (Wu and Huang 2012):

$$q_i = \cos(\beta_i) \cdot S_0 \quad (20)$$

where  $\beta_i$  is the angle between the sunlight and the normal direction of the  $i$ -th surface of the satellite. Given the data of sunlight incidence angle and lightening factor from the orbit discipline, the extreme external heat flux of the satellites over the year can be obtained.

In engineering practices, a number of approaches have been developed to compute the temperature of satellites, e.g., finite element based thermal analysis using commercial software such as SINDA, thermal network analysis, and empirical equations. To balance the analysis accuracy and computational cost for the preliminary design of satellite constellation system, the thermal network analysis method is employed to determine the steady-state temperature inside the satellite. Considering the extreme orbital heat flux and the internal heat source, a thermal network model is established based on several assumptions, i.e., 1) the complex heat conduction inside the satellite is neglected; 2) the space background radiation is neglected; and 3) only the inside part

of satellite has heat conduction to the other panels. Based on the assumptions, the thermal network model consists of seven nodes, i.e., inside part of the satellite (Node 0), south panel (Node 1), north panel (Node 2), top panel (Node 3), bottom panel (Node 4), east panel (Node 5), and west panel (Node 6). Without considering the thermal capacity of MIL, the thermal balance equation of the seven nodes is formulated in (21) (Wu and Huang 2012):

$$\varepsilon_i \sigma A_i T_i^4 + \frac{A_i \lambda_i (T_i - T_0)}{\delta_i} - \alpha_i \bar{q}_i A_i = 0 \quad (21)$$

where  $\sigma = 5.67 \times 10^{-8} \text{ W} \cdot \text{m}^{-2} \cdot \text{K}^{-4}$  is the Stefan–Boltzmann constant, and for the  $i$ -th node,  $T_i$  is the temperature,  $\varepsilon_i$  and  $\alpha_i$  are the surface emissivity and absorption factor respectively,  $A_i$  is the surface area, noted that  $A_{1,2} = A_r$  is the area of each radiator,  $\lambda_i$  is the equivalent thermal conductivity between the  $i$ -th node and Node 0,  $\delta_i$  is the surface thickness, and  $\bar{q}$  is the average extreme heat flux on surface. The associated thermal parameters of each node in this study are referred from (Wu and Huang 2012) and exhibited in the Appendix. Then the thermal balance equation inside the satellite is formulated in (22) (Wu and Huang 2012):

$$cm \frac{dT_0}{dt} = \sum_{i=1}^6 \frac{A_i \lambda_i (T_i - T_0)}{\delta_i} + Q_h \quad (22)$$

where  $c = 300 \text{ J/K/kg}$  is the specific heat of the satellite,  $m$  is the satellite mass, and  $Q_h$  is the internal power dissipation. In this work,  $Q_h$  is set up to be 60% of the power of the satellite output by the power discipline. By solving Eqs. (21) and (22), the maximum temperature in the lightening time is calculated as the local constraint of TC discipline, i.e., less than 303.15 K that works for most devices inside the satellite according to (Wertz 1999). The design variables and constraints of the TC discipline are summarized in Table 5.

### 3.7 Structure discipline

For the structure discipline, the natural frequencies of the satellite are computed as the local constraints of the MDO problem (Wu et al. 2013b). In preliminary design, the natural frequencies can be empirically estimated by regarding the satellite as a simple cantilever, or computed by finite element models. According to (Wu et al. 2013b), high-fidelity



structural FEA models can improve the reliability and practical significance of the optimized results for the spacecraft MDO problems. Thus, a FEA model of the satellite is established in the structure discipline to compute the structural mass and the natural frequencies in this study.

The satellite FEA model contains 4837 nodes and 4982 shell elements, which are exhibited in Fig. 6. In this model, the joint ring is made of aluminum alloy and fixed on the bottom, and the material of fuel tank is titanium alloy. All of the plates in the satellite are made of aluminum honeycomb sandwich material and different plates are connected rigidly to each other. The coupling inputs of the structure discipline are the mass of other subsystems, and they are modeled by the non-structural mass (NSM) on the corresponding plates. The solar arrays are simulated by two concentrated masses at the center of north/south panels. The mechanical parameters of the sandwich material are listed in the Appendix.

The design variables of the structure discipline are the honeycomb core thickness and the ply thickness of the structural plates, and the constraints are the first order bending frequencies around the body-fixed X and Y axes, i.e. no less than 20 Hz according to the requirement of launch vehicle as summarized in Table 6.

### 3.8 Mathematical formulation of the MDO problem

According to the aforementioned disciplinary models, the mathematical formulation of the satellite constellation system MDO problem is finally given by (23), where the symbols have been defined in the multidisciplinary modeling process. In this equation,  $X_c$  is the continuous design variables from different disciplines, while  $X_d$  is the discrete design variables, i.e., the number of orbit planes and the number of satellites in each orbit plane. (23) depicts that the design variables are optimized to obtain a feasible design with the lowest system mass. The optimization problem in (23) is computational-intensive due to the expensive simulation models (e.g., FEA model) and the multidisciplinary design analysis (MDA) iteration process. To reduce the computational cost, a novel surrogate-based optimization method is employed to efficiently solve the satellite constellation system MDO problem, which is detailed in Section 4.

$$\min M_{\text{system}} = (m_{\text{payload}} + m_{\text{power}} + m_{\text{thermal}} + m_{\text{structure}} + m_{\text{others}}) \times P \times S$$

where  $X_c = [h, i, \Omega_0, D_p, f_p, A_s, C_s, T_H, T_P]$ ,  $X_d = [P, S]$

$$s.t \begin{cases} C_R \geq 0.8 \\ R_p \leq 250\text{m}, SNR \geq 500 \\ DOD \leq 0.3, g_w \geq 0 \\ T_0 \leq 303.15\text{K} \\ f_x \geq 20\text{Hz}, f_y \geq 20\text{Hz} \end{cases} \quad (23)$$

## 4 SRBF-SVM for mixed variable optimization

The satellite constellation MDO problem is computationally expensive due to the employment of computation-intensive simulation models (e.g., FEA model). Besides, both continuous and discrete variables need to be handled during the optimization, which further increases the complexity of this MDO problem. To address the challenges, a novel discrete-continuous variable sampling method is incorporated with our previously proposed SRBF-SVM method (Shi et al. 2016) to effectively solve the satellite constellation MDO problem. The novel SRBF-SVM for optimization of mixed discrete and continuous variables is denoted as SRBF-SVM-DC, which is detailed as follows.

### 1) Discrete-continuous variable sampling method

In SRBF-SVM-DC, sample points are initially generated by the Latin hypercube design (LHD) method within the design space of  $R^n \in [0, 1]$ . Based on the discrete variable handling mechanism proposed in (Kleijnen et al. 2010), a discrete-continuous variable sampling method is utilized to map the LHD points to the actual mixed-integer design space of the satellite constellation system MDO problem.

The design variables of mixed-integer optimization problems are given by (24)

$$x = [x_i^c, x_j^d] \quad (24)$$

$i = 1, 2, \dots, n_c, j = 1, 2, \dots, n_d$

where  $x_i^c$  is the  $i$ -th continuous variable,  $x_j^d$  is the  $j$ -th discrete variable, and  $n_c$  and  $n_d$  are the number of continuous and discrete design variables respectively.

As for the continuous variables (e.g., the orbit altitude), the mapping is given in (25)

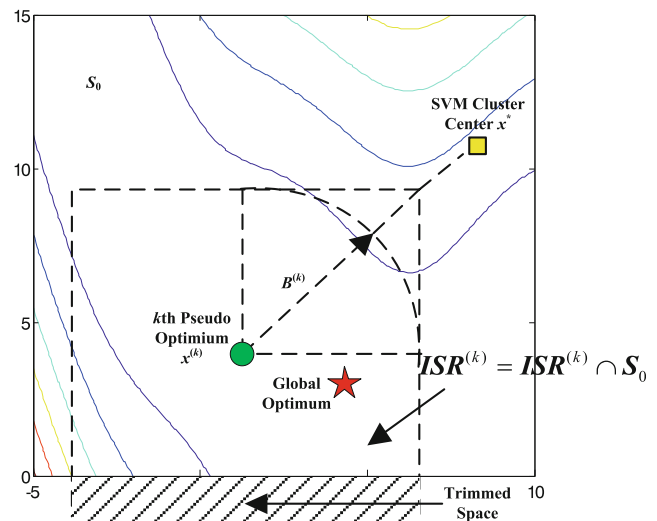


Fig. 7 Illustration of ISR

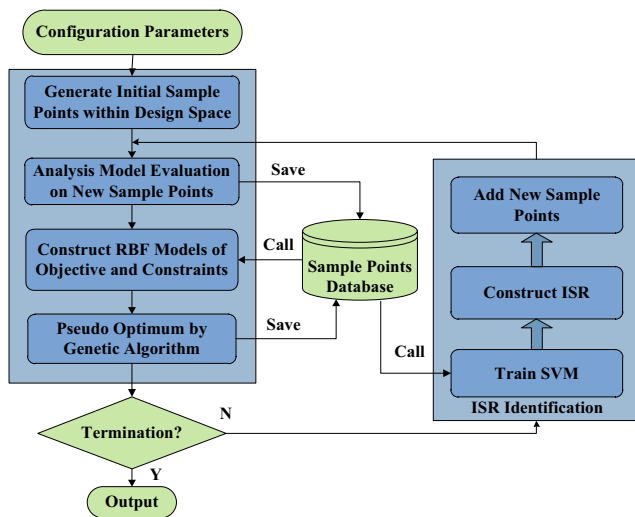


Fig. 8 Flowchart of SRBF-SVM-DC

$$x_i^c = (UB_i - LB_i) \times \bar{x}_i + LB_i \tag{25}$$

where  $\bar{x}_i \in [0, 1]$  is the associated component value of the original LHD points,  $LB_i$  and  $UB_i$  are respectively the lower and upper bounds of  $x_i^c$ .

As for the discrete variables (e.g., the number of orbit planes and satellites), the index of the  $j$ -th discrete variable  $x_j^d$  is first determined according to (26)

$$Index_j = \max \left( 1 + \text{floor} \left( m_j \times \bar{x}_j \right) - \varepsilon, 1 \right) \tag{26}$$

where  $\text{floor}(\cdot)$  represents rounding up to the nearest low integer,  $m_j$  is the associated number of candidate values for  $x_j^d$ ,  $\bar{x}_j \in [0, 1]$  is the associated component value of the original LHD points,  $\varepsilon$  is a sufficiently small number (i.e.,  $10^{-6}$  in this work) to prevent the index from exceeding  $m_j$ .

In the mixed-integer optimization problems, the discrete candidate value set of  $x_j^d$  is given by (27):

$$X_{d,j} = \left[ d_j^{(1)}, d_j^{(2)}, \dots, d_j^{(m_j)} \right] \tag{27}$$

where  $d_j^{(k)}$ ,  $k = 1, 2, \dots, m_j$  is the  $k$ -th candidate value of  $x_j^d$ . Then the discrete variables can be mapped according to the associated indexes as shown in (28).

$$x_j^d = d_j^{(Index_j)}, Index_j = 1, 2, \dots, m_j \tag{28}$$

## 2) Interesting sampling region

Interesting sampling region (ISR) is a relatively small hypercube sub-region where the global optimum is probably located. During the optimization of SRBF-SVM-DC, the RBF surrogates are updated by sequentially adding new sample points in ISR to improve the approximation accuracy of RBF surrogates in the vicinity of the global optimum, which leads the surrogate-based optimization process to the global optimum with higher probability and less computational cost. ISR can be mathematically expressed by (29) (Shi et al. 2016):

$$ISR^{(k)} = \left[ \mathbf{x} \mid \mathbf{x}^{(k)} - \mathbf{B}_k \leq \mathbf{x} \leq \mathbf{x}^{(k)} + \mathbf{B}_k \right] \tag{29}$$

$$\mathbf{B}^{(k)} = \eta \|\mathbf{x}^* - \mathbf{x}^{(k)}\|, \mathbf{1}^T = [1, 1, \dots, 1]_{n_v \times 1}$$

where the pseudo optimum  $\mathbf{x}^{(k)}$ , i.e., the current optimum at the  $k$ -th iteration, is the center of ISR,  $\mathbf{x}^*$  is the cluster center of superior cheap points,  $\mathbf{B}^{(k)}$  is the boundary vector determined by the distance between  $\mathbf{x}^{(k)}$  and  $\mathbf{x}^*$ , and  $\eta$  is the shrinking coefficient used to control the size of  $\mathbf{B}^{(k)}$ .

Table 7 Optimized designs from SRBF-SVM-DC and ICGA

Design variable	Symbol	Unit	Type	Range	ICGA	SRBF-SVM-DC
Orbit altitude	$h$	km	Continuous	[500,1500]	1184.1	1243.3
Orbit inclination	$i$	Deg	Continuous	[30,60]	46.3	44.4
RAAN of the 1st orbit	$\Omega_o$	Deg	Continuous	[0,30]	18.8	29.4
Aperture size of payload	$D_p$	mm	Continuous	[5, 15]	10.7	8.6
Focal length of payload	$f_p$	mm	Continuous	[10,50]	47.8	50.0
Area of solar arrays	$A_s$	m <sup>2</sup>	Continuous	[3, 8]	4.04	4.8
Battery capacity	$C_s$	Ah	Continuous	[20,80]	29.9	20.0
Area of radiators	$A_R$	m <sup>2</sup>	Continuous	[0.5,1.08]	1.08	0.73
Thickness of honeycomb core	$T_H$	mm	Continuous	[7, 13]	10.9	8.4
Thickness of the ply	$T_p$	mm	Continuous	[0.07,0.13]	0.107	0.104
Number of orbit planes	$P$	–	Discrete	[2–6]	4	3
Number of satellite in each plane	$S$	–	Discrete	[1–4]	4	4

**Table 8** Constraint values of the optimized design from SRBF-SVM-DC and ICGA

Constraint	Symbol	Unit	Range	ICGA	SRBF-SVM-DC
Coverage ratio	$C_R$	–	$\geq 0.8$	0.81	0.80
Resolution of payload	$R_P$	m	$\leq 250$	247.9	248.7
Signal to noise ratio of payload	$SNR$	–	$\geq 500$	951.2	567.3
Depth of discharge	$DOD$	–	$\leq 0.3$	0.10	0.15
Power surplus	$g_w$	W	$\geq 0$	33.94	152.3
Maximum temperature	$T_0$	K	$\leq 303.15$	276.6	279.5
1st order bending frequency around X axis	$f_X$	Hz	$\geq 20$	25.4	25.2
1st order bending frequency around Y axis	$f_Y$	Hz	$\geq 20$	28.5	27.3

The identification of ISR can be graphically illustrated in Fig. 7 (Shi et al. 2016). To identify the ISR, a SVM classifier is first trained based on the existing sample points according to (30)

$$\hat{y}_i = \begin{cases} 1 & y_i \leq P_{\text{thresh}} \\ -1 & y_i > P_{\text{thresh}} \end{cases} \quad (30)$$

where  $\hat{y}$  and  $y_i$  are respectively the classification index and objective value of the  $i$ -th sample point,  $P_{\text{thresh}}$  is the classification threshold determined by the objective responses of the existing sample points. Then a large number of points, termed cheap points, are generated by LHD in the design space and classified by the trained SVM. If the predicted classification index is 1, the cheap point is regarded as a superior cheap point, and the cluster center of all the superior cheap points are determined via the feature space fuzzy c-means method (FS-FCM) (Shi et al. 2016). Thus far, the ISR can be successfully identified via (29). The ISR identification algorithm is presented in the Appendix, and more details of ISR are presented in (Shi et al. 2016).

3) Procedure of SRBF-SVM-DC

The overall procedure of SRBF-SVM-DC is illustrated in Fig. 8, which are briefly introduced as follows.

Step 1: The initial parameters of SRBF-SVM-DC are configured including the continuous and discrete design variables, number of initial sample points  $n_s$ ,

**Table 9** System mass of the optimized design from SRBF-SVM-DC and ICGA

Parameters	ICGA	SRBF-SVM-DC
Mass of a single satellite	330.4 kg	314.5 kg
Entire mass of the satellite constellation system	5287.2 kg	3773.3 kg
NFE	>2000	300

newly added sample points  $n_a$  at each iteration, objective, and constraints of the optimization problem. The iteration index  $k$  is set to be 1.

Step 2: Sample points are generated by the aforementioned discrete-continuous variable sampling method within the initial design space. The associated responses including the objective and constraints of the sample points are obtained by evaluating the simulation models.

Step 3: RBF surrogates of the objective and constraints are respectively constructed or updated based on the existing sample points and their associated response values. The construction method of RBF is presented in the Appendix. Then Genetic algorithm (GA) is utilized to conduct global optimization on current RBF surrogates. Note the samples with discrete variables need to be mapped to the actual mixed-integer design space via the aforementioned discrete-continuous variable sampling method before evaluating the fitness function at each generation. In the same way, the current optimum obtained by GA is also mapped to the mixed-integer variable space, which is set as the pseudo optimum  $\mathbf{x}_{\text{opt}}^{(k)}$ . The associated objective and constraints at  $\mathbf{x}_{\text{opt}}^{(k)}$  are evaluated and added to the existing sample pool.

Step 4: If the number of function evaluations exceeds the predefined maximum value, SRBF-SVM-DC is terminated and the current optimal feasible solution is output; otherwise, the procedure continues.

Step 5: Based on the current  $\mathbf{x}_{\text{opt}}^{(k)}$ , the interesting sampling region (ISR) for the next iteration is identified. The ISR identification algorithm is detailed in the Appendix. Then  $n_a$  sample points are generated by the discrete-continuous variable sampling method within the ISR to refine the RBF models, which leads the search to the feasible optimum. Then set  $k = k + 1$ , and the procedure turns to **Step 3** to continue the optimization.

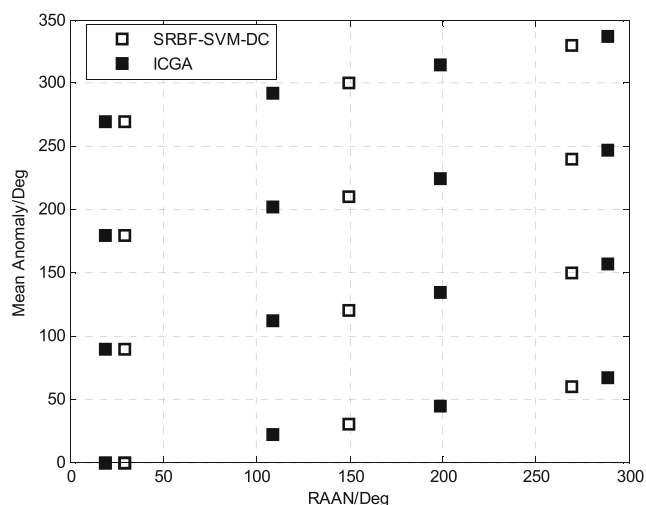


**Fig. 9** Comparison of the satellite distributions from SRBF-SVM-DC and ICGA

## 5 Satellite constellation system optimization results

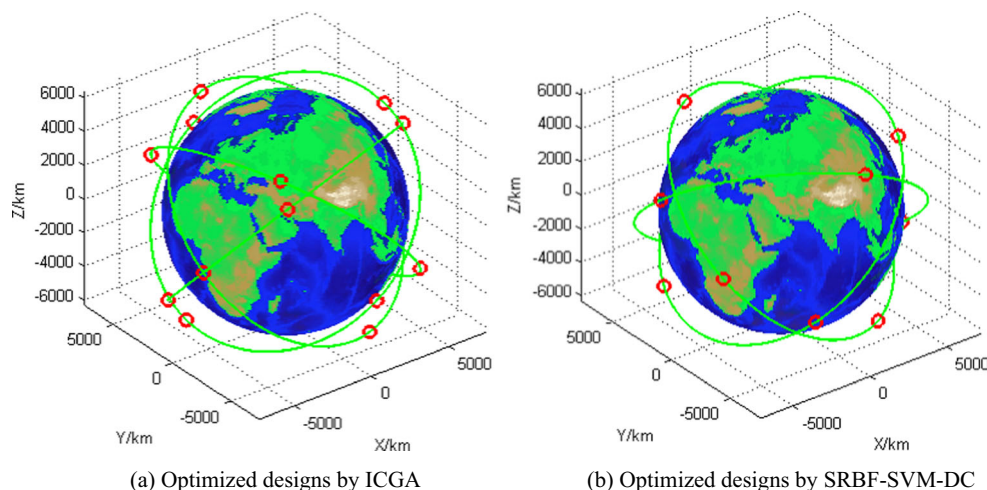
As mentioned above, the satellite constellation system MDO problem in this study is a challenging expensive black-box optimization problem with both continuous and discrete variables. Our proposed SRBF-SVM-DC method is employed to solve the satellite constellation system MDO problem in this section. In view of the global exploration and gradient-free merits for solving black-box optimization problems, genetic algorithm (GA) has been widely employed for constellation optimization in the literatures (Meng et al. 2018; Savitri et al. 2017; Kim et al. 2017). Hence, an integer coding genetic algorithm (ICGA) from MATLAB native *ga* toolbox is also utilized to solve the same satellite constellation MDO problem for comparison.

Considering the limited computational budget, the maximum generation number of ICGA is set as 10, and other

tuning parameters of ICGA (e.g., population size) are set as the default values. In this study, the number of initial sample points is 60, and the number of newly-added sample points at each iteration is six for SRBF-SVM-DC. To balance the optimization efficiency and global exploration capability of SRBF-SVM-DC, the maximum number of function evaluations is set as 300. The optimized design variables from ICGA and SRBF-SVM-DC are listed in Table 7, and the associated constraints of the optimum are summarized in Table 8. The objective values (i.e., the entire mass of the satellite constellation system) and associated NFE from ICGA and SRBF-SVM-DC are compared in Table 9.

The satellites distributions of the optimized designs from SRBF-SVM-DC and ICGA are graphically displayed in Fig. 9, and the associated constellation configurations are illustrated in Fig. 10. The constraint results in Table 8 indicate that the optimized design from SRBF-SVM-DC is feasible (i.e., all the constraints are satisfied) and better refined than that from ICGA. According to Table 7, the number of satellites in each plane from SRBF-SVM-DC is not changed compared with ICGA, while the number of orbit planes is cut down by one. Hence, four satellites are saved in the constellation, which clearly reduces at least 25% of the total mass of the satellite constellation system. However, the altitude of the constellation from SRBF-SVM-DC is increased by 59.2 km to compensate the loss of coverage performance due to the reduced number of satellites, and the associated inclination and RAAN are also relatively adjusted. The increased orbit altitude also yields a larger focus length of the payload to satisfy the resolution constraint, which enlarges the mass budget of the payload. Hence, the aperture size of the payload is correspondingly narrowed to decrease payload mass at the cost of a lower SNR value compared with that of ICGA. The battery capacity and area of radiators from SRBF-SVM-DC are also

**Fig. 10** Illustration of the optimized constellation configurations from SRBF-SVM-DC and ICGA



(a) Optimized designs by ICGA

(b) Optimized designs by SRBF-SVM-DC

decreased to reduce the mass of satellite system, while the area of solar arrays is increased considering different lightning conditions of the orbit. Besides, the thicknesses of the honeycomb core and ply of the structural plates in SRBF-SVM-DC are decreased respectively to yield a lighter structural mass compared with ICGA. Although the structural stiffness of the satellite is relatively weakened, the natural frequency constraints are still satisfied owing to the reduced non-structural mass from other disciplines. Via the aforementioned optimization, the mass of a single satellite from SRBF-SVM-DC is about 16 kg lower than that from ICGA as shown in Table 9, and the entire mass of the satellite constellation system is significantly decreased by about 28.63%, which indicates that the proposed SRBF-SVM-DC yields better global optimum than ICGA. Moreover, the required computational cost of SRBF-SVM-DC is less than 15% of that of ICGA according to Table 9, which is a significant merit in engineering practices when the computational budget is limited.

In summary, the investigations above indicate that the proposed SRBF-SVM-DC is more favorable than the conventional ICGA for satellite constellation MDO problem in terms of both global convergence and efficiency. Via SRBF-SVM-DC optimization, the total mass of the satellite constellation system can be significantly reduced to save the launch and deployment cost, which produces considerable economic benefits from the customers' perspective. Hence, the proposed SRBF-SVM-DC is proved to be feasible and effective to solve the satellite constellation system MDO problem compared with the conventional numerical optimization technique in practice, which can significantly improve the overall design quality and enhance the optimization efficiency. On the other hand, it should be noted that the optimized design might also impose potential challenges for the satellite constellation system. For instances, the decreased numbers of orbit planes and operating satellites increase the risk of the constellation system, i.e., the failures of several satellites in orbits could cause a significant performance reduction of constellation or even the failure of aerospace mission; the weakened structure might breakdown when suffering from unpredictable extraordinary loads. After the preliminary design study in this paper, those challenges are expected be addressed in further detailed design of the satellite constellation system.

## 6 Conclusions

In this paper, a satellite constellation system MDO problem is investigated to minimize the system mass by simultaneously optimizing the parameters of

constellation and individual satellites. Considerable efforts are spent on the multidisciplinary modeling, which is a new endeavor considering the inter-coupling between constellation configuration and satellite subsystems. The constellation model is established based on Walker- $\delta$  configuration, and the coverage ratio for the observation region of interests is computed as the local constraint. As for the small satellites within the constellation, the disciplinary models of CCD payload, power, thermal control, and structure disciplines are established based on different analysis methods, e.g., thermal network for maximum temperature during the lightning period, finite element method for satellite natural frequency, etc. To efficiently solve the computation-intensive satellite constellation MDO problem involving both continuous and discrete variables, a novel SRBF-SVM-DC method is developed based on the SRBF-SVM. In this method, the RBF models of the objective and constraints are respectively constructed and updated in ISR for optimization, which leads the search to converge to the feasible optimum efficiently. In addition, a discrete-continuous variable sampling method is utilized to handle the discrete design variables. In the end, the proposed SRBF-SVM-DC is utilized to solve the studied satellite constellation MDO problem and compared with the conventional ICGA. The optimization results indicate that the optimized total mass of the satellite constellation system from SRBF-SVM-DC is reduced by 28.63% compared with that from ICGA. Moreover, the required computational cost of SRBF-SVM-DC is only 15% of that of ICGA. In conclusion, the study illustrates that the satellite constellation system MDO work is feasible and effective to improve the design quality and reduce the system expenses, and it is highly desirable to apply MBDO techniques to solve the MDO problem with much less computational cost compared with conventional evolutionary algorithms. Furthermore, this surrogate-based satellite constellation system MDO methodology can be applied for other aerospace constellation system design problems, e.g., navigation constellation considering the index of GDOP and mass, which is our future work.

**Acknowledgements** This work was supported by National Natural Science Foundation of China (Grant No. 51675047, 11372036), Aeronautic Science Foundation of China (Grant No. 2015ZA72004), Fundamental Research Fund of Beijing Institute of Technology (Grant No. 20130142008), and Natural Science and Engineering Research Council (NSERC) of Canada (Grant No: R611512 WANG, G-RGPIN04291). The lead author also would like to thank China Scholarship Council (CSC) for their financial support for his study in SFU (Grant No. 201706030009).

## Appendix

### Thermal network model parameters (Wu and Huang 2012)

**Table 10** Parameters of thermal network model

Symbol	Value	Symbol	Value
$\varepsilon_1, \varepsilon_2$	0.86	$A_5, A_6$	$8.5\text{m}^2$
$\varepsilon_3 \sim \varepsilon_6$	0.67	$\lambda_1, \lambda_2$	$1.7 \text{ W}\cdot\text{m}^{-1}\cdot\text{K}^{-1}$
$\alpha_1, \alpha_2$	0.27	$\lambda_3 \sim \lambda_6$	$1.47 \times 10^{-4} \text{ W}\cdot\text{m}^{-1}\cdot\text{K}^{-1}$
$\alpha_3 \sim \alpha_6$	0.35	$\delta_1, \delta_2$	20 mm
$A_3, A_4$	$5\text{m}^2$	$\delta_3 \sim \delta_6$	5 mm

### Structural FEA model parameters

**Table 11** Material parameters for FEA model

Structure	Young's module, Poison ratio, and density
Joint ring	$E = 70.6\text{GPa}, \nu = 0.33, \rho = 2800\text{kg}/\text{m}^3$
Sandwich ply	$E = 70.6\text{GPa}, \nu = 0.33, \rho = 2780\text{kg}/\text{m}^3$
Sandwich core	$E_{11} = E_{22} = 34.9\text{kPa}, \nu = 0.33, G_{12} = 5238\text{Pa}, G_{23} = 55.1\text{MPa}, G_{13} = 36.7\text{MPa}, \rho = 42\text{kg}/\text{m}^3$
Fuel tank	$E = 101.8\text{GPa}, \nu = 0.41, \rho = 4420\text{kg}/\text{m}^3$

### Radial basis function surrogate

Radial basis function (RBF) is an interpolation method on the acquired information at discrete sample points  $\mathbf{x}_k$  (Gutmann 2001). A RBF surrogate can be formulated as

$$\hat{y} = \beta^T \phi(\mathbf{x})$$

$$\phi(\mathbf{x}) = [\phi(\|\mathbf{x}-\mathbf{x}_1\|) \quad \phi(\|\mathbf{x}-\mathbf{x}_2\|) \quad \dots \quad \phi(\|\mathbf{x}-\mathbf{x}_{n_s}\|)]^T \quad (\text{A1})$$

$$\beta = [\beta_1 \quad \beta_2 \quad \dots \quad \beta_{n_s}]^T$$

where  $n_s$  is the number of sample points,  $\phi(\|\mathbf{x}-\mathbf{x}_i\|), i = 1, 2, \dots, n_s$  is radial basis function and  $\beta$  is the coefficient vector of RBF.

Since RBF should satisfy the interpolation condition at sample points, (A1) can be written as

$$\mathbf{A}\beta = \mathbf{y} \quad (\text{A2})$$

where the matrix  $\mathbf{A}$  is the radial basis function matrix shown as below

$$\mathbf{A} = \begin{bmatrix} \phi(\|\mathbf{x}_1-\mathbf{x}_1\|) & \dots & \phi(\|\mathbf{x}_1-\mathbf{x}_{n_s}\|) \\ \vdots & \ddots & \vdots \\ \phi(\|\mathbf{x}_{n_s}-\mathbf{x}_1\|) & \dots & \phi(\|\mathbf{x}_{n_s}-\mathbf{x}_{n_s}\|) \end{bmatrix}_{n_s \times n_s} \quad (\text{A3})$$

The vector  $\mathbf{y}$  consisting of the actual response values at sample points is formulated as

$$\mathbf{y} = [y_1 \quad y_2 \quad \dots \quad y_{n_s}]^T \quad (\text{A4})$$

Coefficient vector  $\beta$  can be calculated as

$$\beta = \mathbf{A}^{-1}\mathbf{y} \quad (\text{A5})$$

Commonly-used radial basis functions can be found in (Wu et al. 2013b).

### Support vector machine

Support vector machine (SVM) developed by Vapnik has been widely used for pattern classification problems (Burges 1998). Consider a group of training samples belonging to two different classes

$$(\mathbf{x}_1, y_1), \dots, (\mathbf{x}_l, y_l), \mathbf{x}_i \in \mathbf{R}^n, y_i \in \{+1, -1\} \quad (\text{A6})$$

where  $\mathbf{x}_i$  is the  $i$ -th sample point,  $y_i$  is the discrete classification value at sample point  $\mathbf{x}_i$ , and  $l$  is the number of training samples.

First, assume that the training samples could be separated linearly by a hyperplane as shown in (A7)

$$(\mathbf{w} \cdot \mathbf{x}) + b = 0, \mathbf{w} \in \mathbf{R}^n, b \in \mathbf{R} \quad (\text{A7})$$

where  $\mathbf{w} = [w_1, w_2, \dots, w_n]$  is the coefficient vector of the hyperplane. The optimal hyperplane can be obtained by solving the constrained convex quadratic optimization problem in (A8), and the equation can be rewritten in (A9).

$$\min \frac{1}{2} \|\mathbf{w}\|^2 \quad (\text{A8})$$

$$s.t \quad g_i = y_i((\mathbf{w} \cdot \mathbf{x}_i) + b) \geq 1, i = 1, \dots, l$$

$$\min \sum_{i=1}^l \alpha_i - \frac{1}{2} \sum_{i,j=1}^l \alpha_i \alpha_j y_i y_j (\mathbf{x}_i \cdot \mathbf{x}_j)$$

$$\alpha_i \geq 0, i = 1, \dots, k \quad (\text{A9})$$

$$s.t \quad \sum_{i=1}^l \alpha_i y_i = 0$$

In (A9),  $\alpha_i$  is the Lagrange multiplier of constraint  $g_i$ , which is obtained by solving the dual optimization problem. Then it is easy to obtain  $\mathbf{w}$  and  $b$  (Burges 1998). The classification function of linear SVM classifier is shown in (A10)

$$f(\mathbf{x}) = \text{sgn} \left( \sum_{i=1}^l y_i \alpha_i (\mathbf{x} \cdot \mathbf{x}_i) + b \right) \quad (\text{A10})$$

where  $\text{sgn}(\mathbf{x}) \in \{-1, +1\}$ ,  $\mathbf{x}$  is an arbitrary design point to be classified.

When the training samples cannot be linearly separated by a hyperplane in Euclidean space  $\mathbf{R}^n$ , a nonlinear mapping  $\varphi(\mathbf{x}) : \mathbf{R}^n \rightarrow \chi$  is utilized to achieve the linear classification of training samples in another space, denoted as feature space  $\chi$ . Thus, the optimal hyperplane in the feature space is expressed as

$$\begin{aligned} & \min \frac{1}{2} \|\mathbf{w}\|^2 \\ \text{s.t. } & g_i = y_i((\mathbf{w} \cdot \varphi(\mathbf{x}_i)) + b) \geq 1, i = 1, \dots, l \end{aligned} \tag{A11}$$

The procedure of determining SVM classification function in  $\chi$  is the same as that in Euclidean space  $\mathbf{R}^n$  as shown in (A12).

$$f(\mathbf{x}) = \text{sgn} \left( \sum_{i=1}^l y_i \alpha_i (\varphi(\mathbf{x}) \cdot \varphi(\mathbf{x}_i)) + b \right) \tag{A12}$$

According to Mercer’s conditions, the inner product of nonlinear mapping could be substituted by a certain kind of kernel function  $K(\mathbf{x}, \mathbf{x}_i)$ . Based on Mercer’s conditions, (A12) is rewritten as below. Commonly-used kernel functions can be found in (Burges 1998).

$$f(\mathbf{x}) = \text{sgn} \left( \sum_{i=1}^l y_i \alpha_i K(\mathbf{x}, \mathbf{x}_i) + b \right) \tag{A13}$$

### Algorithm of interesting sampling region

ISR is a relatively small hypercube sub-region where the global optimum probably is located. ISR is determined by the distance between the current pseudo optimum and the cluster center of superior cheap points. The algorithm to identify ISR is exhibited in Appendix Table 12 (Shi et al. 2016).

Table 12 Algorithm of ISR

<b>Algorithm1 Interesting Sampling Region Identification Algorithm</b>
<b>Input:</b> initial design space $\mathcal{S}_0=[\mathbf{L}_0, \mathbf{U}_0]$ ; sample set $\mathbf{X}$ and response set $\mathbf{Y}$ in sample points database; cheap points set $\mathbf{X}_{data}$ ; pseudo optimal point at current iteration $\mathbf{x}^{(k)}$ , shrinking coefficient $\eta$ .
<b>Output:</b> the interesting sampling region for next iteration $\text{ISR}^{(k)}$
<b>Begin</b>
1 $P_{thresh} \leftarrow \text{EvalThreshold}(\mathbf{Y}, \eta)$
2 <b>foreach</b> $\mathbf{x}_i$ in $\mathbf{X}$
3 <b>if</b> $y_i \leq P_{thresh}$
4 $\hat{y}_i = 1$
5 <b>else</b>
6 $\hat{y}_i = -1$
7 <b>end</b>
8 <b>end</b>
9 Classifier $\leftarrow \text{TrainSVM}(\mathbf{X}, \hat{\mathbf{Y}})$
10 $\mathbf{X}_{sup} = \emptyset$
11 <b>while</b> $\mathbf{X}_{sup} \neq \emptyset$
12 <b>foreach</b> $\mathbf{x}_{di}$ in $\mathbf{X}_{data}$
13 <b>if</b> SVMpredict(Classifier, $\mathbf{x}_{di}$ ) = 1
14 $\mathbf{X}_{sup} = \mathbf{X}_{sup} \cup \mathbf{x}_{di}$
15 <b>end</b>
16 <b>end</b>
17 $P_{thresh} \leftarrow P_{thresh} + 0.1 \text{abs}(P_{thresh})$
18 <b>end</b>
19 $\mathbf{x}^* \leftarrow \text{FS-FCM}(\mathbf{X}_{sup})$
20 $B_k \leftarrow \eta \ \mathbf{x}^* - \mathbf{x}^{(k)}\ _2$
21 $\text{ISR}^{(k)} \leftarrow \text{ShrinkDesignSpace}(\mathbf{x}^{(k)}, B_k)$
22 $\text{ISR}^{(k)} = \text{ISR}^{(k)} \cap \mathcal{S}_0$
23 <b>end</b>
24 <b>return</b> $\text{ISR}^{(k)}$

## References

- Arnas D, Casanova D, Tresaco E (2018) 2D necklace flower constellations[J]. *Acta Astronautica* 142:18–28
- Asgarimehr M, Hossainali MM (2014) Optimization of geosynchronous satellite constellation for independent regional navigation and positioning in Middle East region[J]. *Acta Astronautica* 104(1):147–158
- Budianto IA, Olds JR (2000) A collaborative optimization approach to design and deployment of a space based infrared system constellation[C]. *Aerospace Conf Proc 2000 IEEE*. IEEE 1:385–393
- Burges CJC (1998) A tutorial on support vector machines for pattern recognition[J]. *Data Min Knowl Disc* 2(2):121–167
- Casanova D, Avendaño M, Mortari D (2014) Seeking GDOP-optimal flower constellations for global coverage problems through evolutionary algorithms[J]. *Aerosp Sci Technol* 39:331–337
- Chen S (2003) Design and experiment of astronomy ccd camera. China Astronautic Press, Beijing
- Dai G, Wang M (2009) Multi-objective optimization algorithms and application in satellite constellation design, China University of China Press
- Forrester AIJ, Keane AJ (2009) Recent advances in surrogate-based optimization[J]. *Prog Aerosp Sci* 45(1-3):50–79
- Ghosh A, Coverstone V (2015) Optimal cooperative CubeSat maneuvers obtained through parallel computing[J]. *Acta Astronautica* 107:130–149
- Gutmann HM (2001) A radial basis function method for global optimization[J]. *J Glob Optim* 19(3):201–227
- Huang H, An H, Wu W, Zhang L, Wu B, Li W (2014) Multidisciplinary design modeling and optimization for satellite with maneuver capability[J]. *Struct Multidiscip Optim* 50(5):883–898
- Jin R, Chen W, Simpson TW (2001) Comparative studies of metamodelling techniques under multiple modelling criteria[J]. *Struct Multidiscip Optim* 23(1):1–13
- Kim Y, Kim M, Han B, Kim Y, Shin H (2017) Optimum design of an SAR satellite constellation considering the revisit time using a genetic algorithm[J]. *Int J Aeronaut Space Sci* 18(2):334–343
- Kleijnen JPC, Van Beers W, Van Nieuwenhuysse I (2010) Constrained optimization in expensive simulation: novel approach[J]. *Eur J Oper Res* 202(1):164–174
- Long T, Wu D, Guo X, Wang GG, Liu L (2015) Efficient adaptive response surface method using intelligent space exploration strategy[J]. *Struct Multidiscip Optim* 51(6):1335–1362
- Martins JRR, Lambe AB (2013) Multidisciplinary design optimization: a survey of architectures[J]. *AIAA J* 51(9):2049–2075
- Meng S, Shu J, Yang Q, Xia W (2018) Analysis of detection capabilities of LEO reconnaissance satellite constellation based on coverage performance[J]. *J Syst Eng Electron* 29(1):98–104
- Mortari D, Wilkins MP, Bruccoleri C (2004) The flower constellations[J]. *J Astronaut Sci* 52(1):107–127
- Pu M, Wang J, Zhang D, Jia Q, Shao X (2017) Optimal small satellite orbit design based on robust multi-objective optimization method[J]. *Aerosp Sci Technol* 70:339–350
- Queipo NV, Haftka RT, Shyy W, Goel T, Vaidyanathan R, Tucker PK (2005) Surrogate-based analysis and optimization[J]. *Prog Aerosp Sci* 41(1):1–28
- Savitri T, Kim Y, Jo S, Bang H (2017) Satellite constellation orbit design optimization with combined genetic algorithm and semianalytical approach[J]. *Int J Aerospace Eng* 2017
- Shi R, Liu L, Long T, Liu J (2016) Sequential radial basis function using support vector machine for expensive design optimization[J]. *AIAA J* 55(1):214–227
- Shi R, Liu L, Long T, Liu J, Yuan B (2017) Surrogate assisted multidisciplinary design optimization for an all-electric GEO satellite[J]. *Acta Astronautica* 138:301–317
- Sobieski I (1993) Multidisciplinary design optimization: attempt at definition[C]/industry university workshop on multidisciplinary. *Aircr Des*:23–48
- Sobieszczanski-Sobieski J, Haftka RT (1997) Multidisciplinary aerospace design optimization: survey of recent developments[J]. *Structural optimization* 14(1):1–23
- Walker JG (1977) Continuous whole-earth coverage by circular-orbit satellite patterns[R]. Royal aircraft establishment Farnborough, United Kingdom
- Walker MJH (1986) A set of modified equinoctial orbit elements[J]. *Celest Mech Dyn Astron* 38(4):391–392
- Wang W (2017) Peng H. A fast multi-objective optimization design method for emergency libration point orbits transfer between the sun-earth and the earth-moon systems[J]. *Aerosp Sci Technol* 63:152–166
- Wang GG, Shan S (2007) Review of metamodeling techniques in support of engineering design optimization[J]. *J Mech Des* 129(4):370–380
- Wang L, Shan S, Wang GG (2004) Mode-pursuing sampling method for global optimization on expensive black-box functions[J]. *Eng Optim* 36(4):419–438
- Wertz JR (1999) Space mission analysis and design, 3rd edition (space technology library, vol. 8), 3rd ed., Microcosm
- Wu W, Huang H (2012) Analysis and optimization of sso satellite thermal control subsystem. *Spacecr Eng* 21(2):44–49
- Wu B, Huang H, Chen S, Wu W (2013a) Multi-disciplinary design optimization of ocean satellites based on analytical target cascading strategy. *J Astronaut* 34(1):9–16
- Wu W, Huang H, Chen S (2013b) Wu B. Satellite multidisciplinary design optimization with a high-fidelity model. *J Spacecr Rocket* 50(2):463–466
- Xi X (2003) Orbit foundations of low earth orbit spacecraft. National University of Defense Technology Press, Changsha